The role of lnc-MAPKAPK5-AS1 in immune cell infiltration in hepatocellular carcinoma: Bioinformatics analysis and validation

XIANGZHI HU[1,2], DEDONG WANG[1], JINBIN CHEN[3], BOHENG LIANG[1], LIN ZHANG[1], PENGZHE QIN[1] and DI WU[1]

[1]Guangzhou Center for Disease Control and Prevention, School of Public Health, Guangzhou Medical University, Guangzhou, Guangdong 511436, P.R. China; [2]Infectious Disease Control Department, Yidu Center for Disease Control and Prevention, Yidu, Hubei 443300, P.R. China; [3]Guangzhou Key Laboratory for Clinical Rapid Diagnosis and Early Warning of Infectious Diseases, KingMed School of Laboratory Medicine, Guangzhou Medical University, Guangzhou, Guangdong 510180, P.R. China

Received February 23, 2024; Accepted November 18, 2024

DOI: 10.3892/ol.2025.14887

Abstract. The oncogenic and tumor suppressor roles of lnc-MAPKAPK5-AS1 in multiple cancers suggest its complexity in modulating cancer progression. The expression and promoter methylation level of lnc-MAPKAPK5-AS1 in hepatocellular carcinoma (HCC) was investigated through data mining from The Cancer Genome Atlas and Gene Expression Omnibus and its significance in prognosis and immunity was explored. lnc-MAPKAPK5-AS1 was co-expressed with its protein-coding gene MAPKAPK5 in HCC and exhibited upregulation in HCC tissues as a result of hypomethylation of its promoter region. High expression of lnc-MAPKAPK5-AS1 was associated with poor prognosis. Enrichment analysis revealed that lnc-MAPKAPK5-AS1 is involved in immune and metabolic-related pathways. Changes in the expression of lnc-MAPKAPK5-AS1 affected plasma cells, T cells CD4$^+$ memory resting, NK cells, macrophages M0/M1, and mast cells resting in the tumor microenvironment. lnc-MAPKAPK5-AS1 was found to correlate with multiple immune checkpoints. Analysis of the Sangerbox database revealed positive relationships between expression of lnc-MAPKAPK5-AS1, tumor mutational burden and microsatellite instability, which suggested that immunotherapy may be effective in tumors with high expression of lnc-MAPKAPK5-AS1. The expression of lnc-MAPKAPK5-AS1 was verified to indicate sensitivity to 16 common targeted drugs. Immunohistochemistry confirmed the expression of MAPKAPK5 protein in HCC and its prognostic significance. Weighted gene co-expression network analysis was applied to identify hub genes related to both immunoreactive score and gene expression. These results revealed that lnc-MAPKAPK5-AS1 may be involved in the occurrence and development of HCC as an oncogene and may represent a potential therapeutic target through modulating the substance metabolism and immune response.

Correspondence to: Dr Di Wu, Guangzhou Center for Disease Control and Prevention, School of Public Health, Guangzhou Medical University, 1 Xinzao Road, Xinzao Town, Panyu, Guangzhou, Guangdong 511436, P.R. China
E-mail: wudi0729@126.com

Key words: hepatocellular carcinoma, lnc-MAPKAPK5-AS1, MAPKAPK5, prognosis, immune infiltration

Introduction

Primary liver cancer is the fourth most common malignant tumor and the second leading cause of cancer death in China (1). Hepatocellular carcinoma (HCC) is the most common pathological type of primary liver cancer and has a high incidence rate. The incidence rate of HCC in China ranks first in the world, and the annual new HCC cases in China account for ~45% of total new HCC cases worldwide (2). HCC is usually diagnosed at an advanced stage, and conventional radiotherapy, chemotherapy and molecular targeting have not demonstrated satisfactory therapeutic effects. Although liver ultrasonography every 6 months with or without serum alpha-fetoprotein (AFP) level, computerized tomography, and magnetic resonance imaging are currently accepted methods for HCC surveillance, their effectiveness has been controversial due to sex, physical habits, cost and other limitations (3). Moreover, even after surgical treatment, the recurrence rate remains high. The majority of HCC cases in China develop from hepatitis; multiple factors, such as the interaction of multiple inflammatory cells and the formation of tumor angiogenesis, result in an immunosuppressive microenvironment, limiting the clinical efficacy of immune checkpoint inhibitors. As HCC has an insidious onset and difficulty in early diagnosis, timely and effective treatment after diagnosis is essential for inhibiting disease progression. Therefore, there is an urgent need to find new diagnostic and prognostic indicators for HCC. In recent years, immunotherapy drugs have been gradually applied in the clinical treatment of HCC, which has expanded the treatment possibilities for HCC. Therefore, a comprehensive understanding of the immune infiltration in HCC is also particularly important to select the most effective immunotherapy strategy.

Long non-coding RNAs (lncRNAs) are non-coding RNAs >200 nucleotides (4). lncRNAs specifically bind to various

proteins and nucleic acids through their secondary structures. With the development of next-generation sequencing technology and the large amount of high-throughput sequencing data on tumors, these advances have made it possible to predict the function of lncRNAs in tumors using bioinformatics analysis. Previous studies have demonstrated that some tissue-specifically lncRNAs cis-regulate the transcription of adjacent protein-coding genes, and this co-expression pattern has important implications for other biological processes (5). lncRNAs also play key transcriptional regulatory roles by influencing gene expression by recruiting protein complexes or competing for transcription factors. The function of lncRNAs in diseases is closely related to their subcellular localization. Wang *et al* (6) reported that cytoplasmic lnc-IGFL2-AS1 acts as a competing endogenous (ceRNA) to bind microRNA (miRNA or miR)-4795-3p, promoting the expression of IGFL1, while in the nucleus, it promotes the formation of the KLF5/TEAD4 transcriptional complex at the enhancer of IGFL2.

lnc-MAPKAPK5-AS1 (hereinafter referred to as MK5-AS1) is located on chromosome 12:112280206-112282706 with a length of 2,390 nucleotides. It has been demonstrated that it is strongly linked to the clinicopathological characteristics and prognosis of various patients with cancer. Research has revealed that MK5-AS1 is highly expressed in colorectal cancer and can promote the proliferation of cells by inhibiting the expression of p21 (7). Yang *et al* (8) also confirmed the adverse mechanism of MK5-AS1 in colorectal cancer, including the formation of a MK5-AS1-let-7f-1-3p-SNAI1 ceRNA network and cis-regulation of its adjacent gene MAPKAPK5 (henceforth called MK5). Zhang *et al* (9) reported that MK5-AS1 is an independent risk factor for lung adenocarcinoma and silencing its expression has been validated to markedly inhibit the proliferation of lung adenocarcinoma cells. However, there were few studies on the association between MK5-AS1 and the tumor microenvironment (TME) in HCC. Therefore, the role of MK5-AS1 in HCC and its regulatory relationship with downstream target gene MK5 was elucidated in the present study. Furthermore, the role of MK5-AS1 in the immune microenvironment was investigated through multiple public databases by bioinformatics analysis, aiming to provide new clues for individualized treatment of HCC cases.

Materials and methods

Data collection and processing. The transcriptome data of The Cancer Genome Atlas Liver Hepatocellular Carcinoma program '(TCGA)-LIHC' and the corresponding clinical data updated, was downloaded on November 3, 2022 from TCGA (https://portal.gdc.cancer.gov/repository) (10), which contains expression profiles of mRNAs and lncRNAs of patients with HCC. After removing duplicate samples, the expression data of 369 patients with HCC and 50 non-tumor liver patients were obtained and converted into TPM format after preprocessing. The GSE144269 dataset was downloaded from Gene Expression Omnibus (GEO) (https://www.ncbi.nlm.nih.gov/geo/, accessed on November 5, 2022) (11) for validation of gene expression and prognosis. Mutation data of HCC were collected and visualized in R using 'maftools', and the characteristics of the mutation status were investigated.

Correlation analysis of lnc-MAPKAPK5-AS1 expression and clinicopathological factors. The expression patterns of MK5-AS1 and MK5 in HCC tissues and normal tissues from TCGA were compared. GSE144269 was used as an external validation dataset to verify the expression status of the two genes. The 369 patients with HCC were divided into high expression group and low expression group using the medians of MK5-AS1 and MK5, and the relationships between gene expression and clinical parameters were analyzed.

Gene Ontology (GO) functional annotation and Kyoto Encyclopedia of Genes and Genomes (KEGG) pathway enrichment analysis. The expression profiles were compared between the MK5-AS1 high and low expression groups; a total of two sets of differentially expressed genes (DEGs) were obtained from TCGA-LIHC and GSE144269. lncRNAs and mRNAs in both gene sets were screened and imported into Metascape (http://metascape.org, accessed on 19 December 2022) (12) for functional enrichment analysis. KEGG enrichment analysis was performed using the 'clusterProfiler' R package to screen out relevant pathways (13).

Gene Set Enrichment Analysis (GSEA). GSEA (14) was performed using the 'clusterProfiler' R package in the Molecular Signatures Database (MSigDB)_v7.0_GMTs with the reference dataset 'c5.all.v7.0.entrez.gmt'. Significantly altered pathways were validated with 1,000 iterative calculations, and the expression level of MK5-AS1 was considered as a phenotypic marker. According to the reference information of GSEA official software, it is generally considered that the NES absolute value is greater than 1, NOM $P<0.05$, false discovery rate (FDR) q-value <0.25 of the enrichment pathways are significantly enriched between high and low MK5-AS1 expression groups in HCC (15-18).

Immunohistochemistry (IHC) assay. HCC tissue microarrays used for analysis were commercial products purchased from Shanghai Xinchao Biological Technology Co. Ltd. (cat. no. hlivh180su15). All experiments were performed following the manufacturer's instructions. The corresponding clinical information was also provided by the company. The protocol was approved (approval no. SHYJS-CP-1901001 on 11th January 2019, and extended as approval no. SHYJS-BC-2310001 on 20th October, 2023) by the ethics committee of Shanghai Xinchao Biological Technology Co., Ltd. (Shanghai, China). The tissue microarray contained tumor samples from 90 patients with HCC who received surgical treatment from June 2007 to October 2008. Clinical data included HBsAg, anti-hepatitis C (HCV), alanine aminotransferase (ALT), AFP, and other liver indicators, as well as pathological characteristics such as TNM stage and histological grade. The follow-up period was 3 to 5 years, and data on the overall survival (OS) and disease-free survival (DFS) were collected.

Tissue sections were deparaffinized in xylene for 0.5 h twice. The sections were hydrated in ethanol, followed by high-pressure antigen recovery by heating the tissue with EnVision FLEX TARGET RETRIEVAL SOLUTION LOW pH (pH, 6.1, 3 min; cat. no. K8005; Dako; Agilent Technologies, Inc.). Endogenous peroxidase was blocked by incubating the

sections with 3% hydrogen peroxide at room temperature for 15 min. In addition, the sections were blocked with 1X Antibody Diluent/Block (cat. no. ARD1001EA; Akoya Biosciences) at room temperature for 30 min. Subsequently, the slides were stained with a primary antibody against MAPKAPK5 (1:100; cat. no. HPA015515; Atlas Antibodies) at 4˚C overnight. The slides were then incubated with an appropriate HRP-conjugated secondary antibody (EnVision FLEX$^+$, Mouse, High pH; no dilution required; cat. no. SM802; Dako; Agilent Technologies, Inc.) at 37˚C for 30 min. Furthermore, DAB (25˚C, 5 min) and hematoxylin (25˚C, 1 min) were used for visual antibody staining. An optical microscope was used for observation and to capture images. MAPKAPK5 cytoplasmic staining was scored using four grades (0: negative, 1: weakly positive, 2: moderately positive, 3: strongly positive). The percentage of positive cells was categorized into five grades (0: 0%, 1: 1-5%, 2: 6-25%, 3: 26-50%, 4: 51-100%). The final IHC score was calculated as follows: intensity grad x positive cell percentage grade. A score of 0-3 indicated low expression, and a score of 4-9 indicated high expression.

Relationship between lnc-MAPKAPK5-AS1 and the TME. CIBERSORT is an accurate and robust algorithm that calculates the immune cell composition of tumor tissues by the gene expression profiles (13). The normalized mRNA expression matrix of patients with HCC in TCGA was analyzed using the 'CIBERSORT' source R package, which was obtained from the website https://rdrr.io/github/singha53/amritr/src/R/supportFunc_cibersort.R. Other required data were obtained from the supplementary data of a previously published article (13) (https://www.nature.com/articles/nmeth.3337#MOESM207), which included the gene expression matrix for 22 types of immune cells. The number of permutations was 1,000, and the components of various immune cells were compared in MK5-AS1 high and low expression groups. The single sample gene set enrichment analysis (ssGSEA) algorithm was used to assess the infiltration degree of 28 different immune cells. A matrix of immune cell (B cells, CD4$^+$ T cells, CD8$^+$ T cells, neutrophils, macrophages and dendritic cells) infiltration levels of TCGA-LIHC samples were also downloaded using the TIMER database (https://cistrome.shinyapps.io/timer/ (19), accessed on 21 December 2022) and the correlation between the expression status of *MK5-AS1* and immune cell infiltration level in HCC was detected.

Correlation between expression of lnc-MAPKAPK5-AS1 and tumor mutational burden (TMB), microsatellite instability (MSI) and immune checkpoint inhibitors (ICIs). A number of clinical studies have demonstrated an association between TMB, MSI and the effect of immunotherapy (20-22). Therefore, such emerging biomarkers may be implicated in the regulation of TME, therefore the relationship between these biomarkers and the expression of MK5-AS1 were explored. Spearman correlation analysis was conducted using SangerBox (http://vip.sangerbox.com/home.html, accessed on 18 October 2022). The TMB value of patients with HCC and high and low expression of MK5-AS1 was calculated. A boxplot of TMB value was generated to visualize the results using the 'ggbetweenstats' function of 'ggstatsplot' package. Immunotherapy is a strategy for tumor treatment and includes immunotherapy targeting programmed death protein-1 (PD-1)/programmed death protein ligand-1 (PD-L1) and cytotoxic T lymphocyte-associated antigen (CTLA-4). These immunotherapies have demonstrated great efficacy and application prospect in the treatment of advanced HCC (23). Immune checkpoint molecules play an important role in maintaining immune homeostasis and can be exploited for the immune evasion of tumor cells. The relationship between MK5-AS1 and eight immune checkpoints were examined to identify its potential effect in immunotherapy.

Drug susceptibility analysis. The 'pRRophetic' R package, developed by Professors Paul Geeleher, Nancy Cox and R. Stephanie Huang at the University of Minnesota, was designed to predict phenotypes by gene expression data (24). It uses data of the CGP cell line from the Cancer Genome Project to predict clinical outcomes and drug sensitivity of external cell lines (Cancer Cell Line Encyclopedia) (25). The potential chemotherapeutic efficacy of 16 common drugs in HCC was examined on the basis of gene expression profiles in TCGA and the differences in the sensitivity of the drugs between MK5-AS1 high and low expression groups were compared.

Methylation status of the promoter region of lnc-MAPKAPK5-AS1. Diseasemeth 2.0 (http://bio-bigdata.hrbmu.edu.cn/diseasemeth/, accessed on 18 November 2022) (26) was used to examine the methylation pattern of the promoter region of MK5-AS1 and its relation to different clinical stages and histological grades. The somatic mutation data of HCC was downloaded from TCGA and the overall mutation status was analyzed. The results were visualized using the cBioPortal database (http://www.cbioportal.org (27), accessed on 1 February 2023).

Prediction of the relationship between lnc-MAPKAPK5-AS1 and miRNAs. Based on high-throughput sequencing data from 15 cell lines, lncATLAS (http://lncatlas.crg.eu/, accessed on 5 September 2022) (28) was used to collect data of 6,768 lncRNAs and to evaluate specific subcellular localization using the 'relative concentration index'. This database was used to predict the localization of MK5-AS1. Target miRNAs that interact with MK5-AS1 were predicted using the ENCORI platform (http://starbase.sysu.edu.cn/, 5 January 2023) (29), which contains networks of interactions among RNAs. The screening conditions were as follows: i) 'miRNA-Target: miRNA-lncRNA'; ii) 'Genome: human'; and iii) 'Target Gene: lnc-MAPKAPK5-AS1'. The expression of the miRNAs in HCC and the correlation with MK5-AS1 expression using data from TCGA were explored.

Weighted correlation network analysis (WGCNA) screening of key modules and hub genes related to immune activity. WGCNA is an algorithm widely used to identify biomarkers through clustering sets of genes with similar expression patterns (30). It calculates the associations between distinct modules and specific clinical features. A total of 8,900 DEGs were identified from HCC tissues and normal tissues and 5,100 DEGs from the high MK5-AS1 expression group and low MK5-AS1 expression group. A total of 3,255 DEGs were obtained by intersection of the two gene sets. The 'WGCNA'

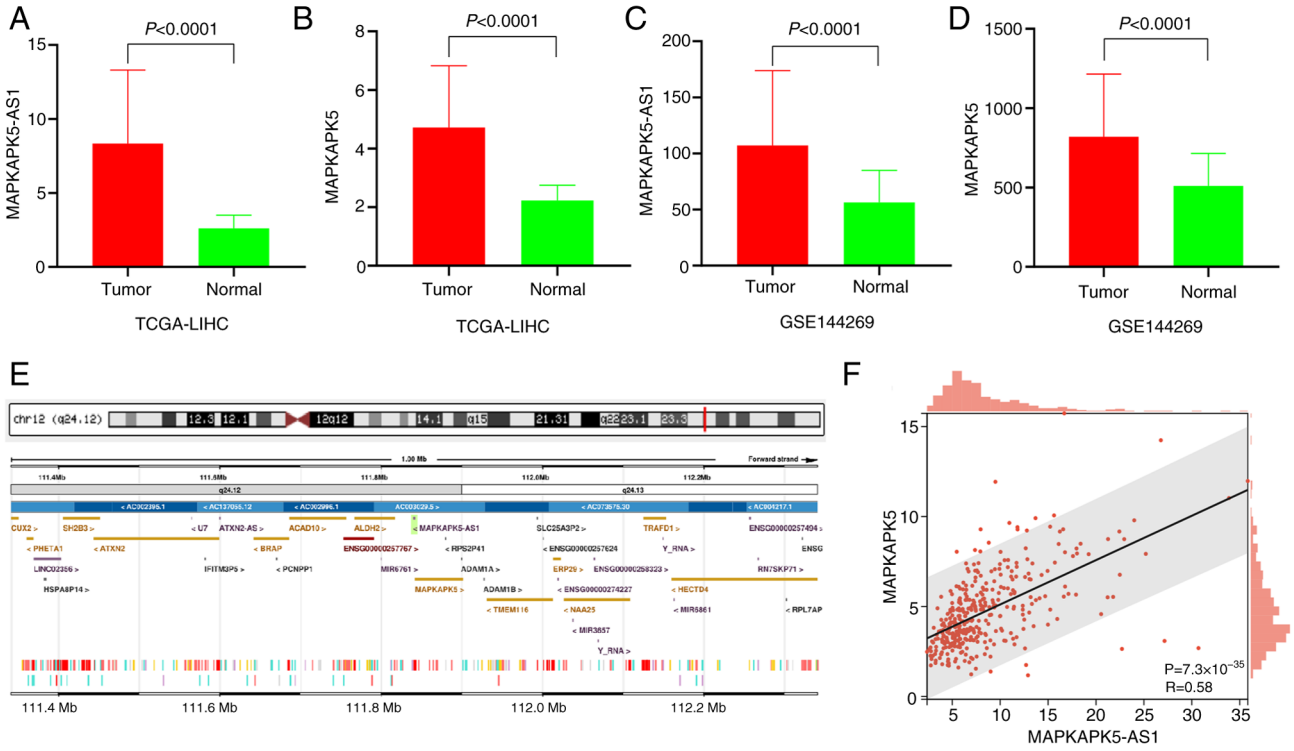

Figure 1. Comparison of lnc-MAPKAPK5-AS1 and MAPKAPK5 expression in HCC and normal liver tissues. (A and B) MK5-AS1 and MK5 have consistent expression pattern in TCGA-LIHC. (C and D) The expression levels of MK5-AS1 and MK5 were upregulated in HCC in Gene Expression Omnibus. (E) The Ensemble Genome browser (http://asia.ensembl.org/) revealed that MK5 was the nearby gene of MK5-AS1. (F) Spearman correlation analysis of MK5-AS1 expression and MK5 expression in TCGA-LIHC. HCC, hepatocellular carcinoma; TCGA-LIHC, The Cancer Genome Atlas Liver Hepatocellular Carcinoma.

R package was applied to construct the co-expression network of 3,255 genes and 369 HCC samples were clustered. β=3 was selected as the soft threshold power to construct the scale-free network. A hierarchical clustering tree was constructed using the dynamic hybrid cutting technology to gather genes with similar expression patterns. The STRING (http://string.embl.de/) (31) database was used to explore the interaction network between proteins, which helps to identify the key regulatory genes.

The cytolytic activity score (CYT) is a robust transcriptome-based immune signature across multiple cancer types and defined as the mean of GZMA and PRF1 expression (TPM format). It has been revealed that a higher CYT is associated with improved outcomes (32).

The IFNG6 score can reflect the overall immune activity and predict the therapeutic effect of pembrolizumab in patients with HCC. This score is calculated from the average expression of six genes (CXCL9, CXCL10, IDO1, IFNG, HLA-DRA and STAT1) (33).

Statistical methods. R-4.1.2 and GraphPad Prism-8.00 were used for data cleaning, statistical analysis and graphing. A Kolmogorov Smirnov test was performed to determine the distribution and then based on that, an unpaired t-test was used to explore the difference in MK5-AS1 expression between the HCC and normal groups in the TCGA-LIHC dataset. As for the GSE144269 dataset, the tumor and normal groups were originated from the same patients and then a paired t-test was used to analyze the differences in MK5-AS1 expression between the aforementioned two groups. The histogram was visualized using the median gene expression with an interquartile range. Kruskal-Wallis test with post hoc test (Dunn's or Steel-Dwass) for multiple testing correction was used for multi-group comparison. The chi-square test and Fisher's exact test were employed in the analysis of the relationship between gene expression and clinicopathological characteristics of patients with HCC. Survival curves were drawn using Kaplan-Meier method and comparison among different groups was performed using the log-rank test. Cox regression models were utilized for univariate and multivariate analysis. The prognostic ability of the two genes was assessed by the area under the ROC curve (AUC). Correlations between genes and immune infiltrating cells were compared using Spearman correlation analysis. Two-sided P<0.05 were considered statistically significant in all analyses. Bonferroni correction was used for pairwise comparisons between multiple groups.

Results

Expression of lnc-MAPKAPK5-AS1 in HCC tissues. As depicted in Fig. 1A and B, the expression levels of MK5-AS1 and MK5 showed significant upregulation in HCC tissues compared with normal liver tissues in TCGA (both P<0.0001). The median with interquartile range of MK5-AS1 in HCC and normal liver tissues was 6.965 and 5.247-10.010 vs. 2.536 and 2.003-3.094, respectively; for MK5, they were 4.268 and 3.199-5.719 vs. 2.180 and 1.870-2.525, respectively. Similar results were observed in the GSE144269 dataset (both P<0.0001, Fig. 1C and D).

Antisense lncRNAs are often correlated with the expression of their sense strand genes, suggesting that they probably be widely involved in the expression regulation of protein-coding genes (5). MK5-AS1 is transcribed from the antisense strand of its protein-coding gene MK5, and the two genes have partially overlapping sequences (Fig. 1E). Spearman's correlation analysis revealed a positive correlation between the two genes (Fig. 1F).

Correlation of gene expression with clinicopathological factors in HCC. The relationship between the expression levels of MK5-AS1 and MK5 and several widely recognized clinicopathological factors was explored. Analysis of UALCAN (http://ualcan.path.uab.edu/, accessed on 20 October 2022) (34) revealed that a higher expression level of MK5-AS1 was associated with higher clinical stage and histological grade of HCC tissues (Fig. 2A and B). The 369 patients with HCC were divided into the high expression groups and low expression groups using the median of gene expression. As shown in Table I, higher expression of MK5-AS1 was significantly associated with advanced clinical stage (χ^2=5.372, P=0.020), T stage (χ^2=5.280, P=0.022), histological grade (χ^2=17.825, P<0.01) and higher AFP (χ^2=29.950, P<0.01). Notably, MK5 exhibited similar tendencies: MK5 expression was negatively linked with the clinical stage (χ^2=4.554, P=0.033), T stage (χ^2=3.983, P=0.046), histological grade (χ^2=17.825, P<0.01) and higher AFP (χ^2=23.348, P<0.01) in patients with HCC (Table II). These findings indicated that high expression of MK5-AS1 and MK5 may be potential risk factors for HCC.

Association between the expression of two genes and the diagnosis and prognosis in patients with HCC. Time-dependent ROC curve analysis revealed that MK5-AS1 had high sensitivity and specificity for the five-year survival rate of patients with HCC (AUC=0.78, Fig. 2C). The AUC of MK5 for predicting five-year survival rate was 0.77 (Fig. 2D). To further examine the relationship between gene expression and survival, Kaplan-Meier survival curves were used to examine the effect of MK5-AS1 expression on the overall survival rate of patients with HCC in TCGA and GEO. The median survival time of patients with HCC with high MK5-AS1 expression in TCGA was only 39 months, while it was ~70 months for patients with low MK5-AS1 expression (P=0.01, Fig. 2E). Analysis of GEO data also suggested that the high expression group had improved survival outcomes (P=0.013, Fig. 2F). The results of the survival analysis of MK5 were consistent with these findings; its high expression was an adverse factor for the prognosis of patients with HCC (P=0.013, P=0.05; Fig. 2G and H).

Cox regression analysis can be used to examine whether the gene expression level is a risk factor that affects survival. Univariate Cox regression analysis showed that compared with patients with low MK5-AS1 and MK5 expression, patients with high expression of MK5-AS1 and MK5 indicated a substantially higher risk of mortality. The variables with a statistically significant effect on survival were further included in multivariate Cox regression analysis. The results revealed that MK5-AS1 and MK5 may be independent risk factors for poor survival when M stage was contained (Table III, Fig. 2I). These results suggested that high expression of MK5-AS1 in patients with HCC was associated with tumor progression and adverse prognosis.

Enrichment analysis of overlapping DEGs in TCGA and GSE144269. Using 'DESeq2' R package, 4,179 and 3,706 differentially expressed lncRNAs and mRNAs (|logFC|≥0.6, FDR <0.25, P<0.05) were identified in the TCGA-LIHC and GSE144269 datasets, respectively. A Venn diagram was plotted to select the intersecting genes of the aforementioned two gene sets and 676 genes co-expressed with MK5-AS1 were finally obtained (Fig. 2J). GO analysis demonstrated that MK5-AS1-related genes were primarily enriched in biological regulation, metabolic progress, response to stimulus, multicellular organismal process and immune system process (Fig. 3A). Based on the functional correlation, a network of enriched terms colored by cluster ID was constructed in accordance with correlation and similarity, where nodes that share the same cluster ID were typically close to each other (Fig. 3B). The relative number of genes in each pathway is demonstrated in Fig. 3C; a darker color indicates a greater number of genes, as observed in the pathway 'biological regulation'. KEGG analysis results suggested that DEGs may be involved in various metabolic-related pathways, such as the PRAK signaling pathway, cell adhesion molecules, carbon metabolism, bile secretion, synaptic vesicle cycle, biosynthesis of amino-acids, complement and coagulation cascades and fatty acid metabolism (Fig. 3D).

GSEA was performed on the basis of normalized enrichment score and the FDR. Regulation of immune system process, biological adhesion, collagen containing extracellular matrix, immune effector process, small molecule metabolic process and defense response were significantly enriched signaling pathways (P<0.05, Fig. 3E).

Relationship between MAPKAPK5 expression at protein level and clinicopathological parameters in HCC tissue chips. To make our results more credible at the histological level, an external validation of the gene expression pattern and prognostic significance from 90 HCC tissue chips was carried out. Immunohistochemical semi-quantitative evaluation of clinicopathological specimens showed that the expression score of MK5 in HCC was significantly higher than that in normal tissues (Fig. 4A and B); the median with interquartile range of MK5 in HCC and normal tissues were 1.067 and 1.000-1.500 vs. 0.811 and 0.500-1.000, respectively. Based on a threshold of P<0.05, it was found that the clinical stage (χ^2=7.701, P=0.006), ALT (χ^2=5.011, P=0.025), and PD-L1 expression (χ^2=7.003, P=0.008) was strikingly associated with the expression level of MK5 (Table IV). Nevertheless, the remaining clinicopathological factors such as sex, age, pathology grade, tumor size, recurrence, HBsAg, HBcAb, AntiHCV, AFP and CTLA4 were not statistically significant. As detailed in Fig. 4C and D, patients with HCC with decreased MK5 expression had longer OS and DFS, which shed light on the probability that MK5 acted as a risk factor in the development of HCC.

Analysis of tumor-infiltrating immune cells. To clarify the relationship between MK5-AS1 and tumor infiltrating immune cells, the association between MK5-AS1 expression and the infiltration levels of six immune cells in HCC was investigated

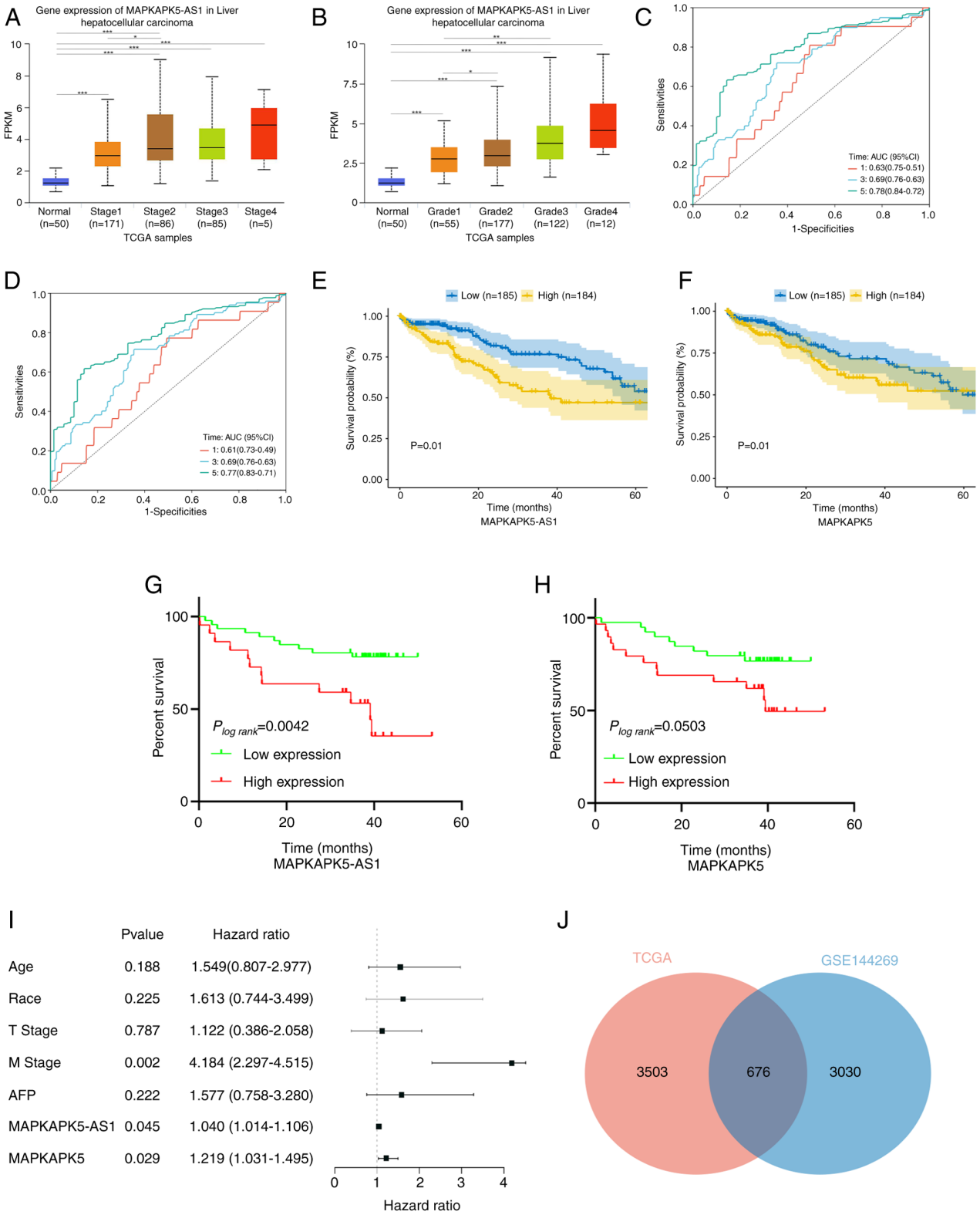

Figure 2. Prognostic analysis of lnc-MAPKAPK5-AS1 and MAPKAPK5 in patients with HCC. (A and B) MK5-AS1 expression is significantly correlated with patients with clinical stages and histologic grades of HCC. (C and D) Receiver operation characteristic curve analysis of the 1-year, 3-year and 5-year survival rates of patients with HCC by MK5-AS1 and MK5. (E and F) Differences in survival among high and low MK5-AS1 levels in TCGA and GEO. (G and H) Overall survival analysis of MK5 in TCGA and GEO. (I) Multivariate Cox analysis of MK5-AS1 expression and other clinicopathological factors using a forest plot. (J) Venn plot of the intersection of differentially expressed genes in TCGA-LIHC and GSE144269. HCC, hepatocellular carcinoma; TCGA, The Cancer Genome Atlas; LIHC, Liver Hepatocellular Carcinoma; GEO, Gene Expression Omnibus; GSE, Gene Set Enrichment.

using the immune cell infiltration data downloaded from the TIMER online database. All correlation analysis conducted with Spearman's test exhibited statistically significant positive correlations, including B cells (R=0.20, P=1.1x10^{-4}), CD4^{+} T (R=0.31, P=8.9x10^{-10}), CD8^{+} T (R=-0.10, P=0.07), neutrophils (R=0.31, P=2.9x10^{-9}), macrophages (R=0.34, P=1.5x10^{-9}) and

Table I. Relationship between lnc-MAPKAPK5-AS1 expression and clinicopathological parameters of hepatocellular carcinoma samples in The Cancer Genome Atlas.

Characteristics	n	Expression level of lnc-MAPKAPK5-AS1		χ^2	P-value
		High (n=184)	Low (n=185)		
Sex				0.856	0.355
Male	249	120 (48.2)	129 (51.8)		
Female	120	64 (53.3)	56 (46.7)		
Age, years				0.171	0.679
≤60	177	90 (50.8)	87 (49.2)		
>60	191	93 (48.7)	98 (51.3)		
Ethnicity				0.807	0.668
Asian	158	83 (52.5)	75 (47.5)		
White	182	87 (47.8)	95 (52.2)		
Others	19	10 (52.6)	9 (47.4)		
BMI				1.162	0.281
<24	160	84 (52.5)	76 (47.5)		
≥24	178	83 (46.6)	95 (53.4)		
Historical risk factors				0.738	0.691
Alcohol consumption	117	61 (52.1)	56 (47.9)		
Hepatitis virus	114	53 (46.5)	61 (53.5)		
Others	119	59 (49.6)	60 (50.4)		
Clinical stage				5.372	0.020
I, II	257	118 (45.9)	139 (54.1)		
III, IV	88	53 (60.2)	35 (39.8)		
T				5.280	0.022
T1, T2	275	128 (46.5)	147 (53.5)		
T3, T4	91	55 (60.4)	36 (39.6)		
N					0.364
N0	250	122 (48.8)	128 (51.2)		
N1	4	3 (75.0)	1 (25.0)		
M					0.622
M0	265	134 (50.6)	131 (49.4)		
M1	4	3 (75.0)	1 (25.0)		
Histologic grade				17.825	<0.01
G1, G2	232	96 (41.4)	136 (58.6)		
G3, G4	132	85 (64.4)	47 (35.6)		
AFP				29.950	<0.01
<20	147	51 (34.7)[a]	96 (65.3)[a]		
≥20 and <400	66	31 (46.9)[a]	35 (53.1)[a]		
≥400	65	49 (75.4)[b]	16 (24.6)[b]		
Child pugh grade				0.023	0.880
A	217	95 (43.8)	122 (56.2)		
B, C	22	10 (45.5)	12 (54.5)		
Treatment type				0.024	0.876
Pharmaceutical therapy	184	91 (49.5)	93 (50.5)		
Radiation therapy	185	93 (50.3)	92 (49.7)		

The chi-square test and Fisher's exact test were utilized in the analysis of the relationship between gene expression and clinicopathological characteristics of HCC patients. Kruskal-Wallis test with post hoc test (Dunn's or Steel-Dwass) for multiple testing correction was used for multi-group comparison. In analyzing the differences in RAB11B expression among various patient groups characterized by a specific clinical variable, the letters 'a' and 'b' indicate the presence or absence of a statistically significant difference in RAB11B expression between any two groups. If both groups share the same letter, this signifies no statistical difference; conversely, differing letters denote a statistically significant difference. Several parameters have missing values: 1 in age, 31 in BMI, 19 in history risk factors, 24 in clinical stage, 3 in T stage, 115 in N stage, 100 in M stage, 5 in histologic grade, 91 in AFP, and 130 in child pugh grade. TNM, tumor-node-metastasis; BMI, body mass index; AFP, alpha fetoprotein.

Table II. Relationship between MAPKAPK5 expression and clinicopathological parameters of hepatocellular carcinoma samples in The Cancer Genome Atlas.

Characteristics	n	Expression level of MAPKAPK5		χ^2	P-value
		High (n=184)	Low(n=185)		
Sex				0.167	0.683
Male	249	126 (50.6)	123 (49.4)		
Female	120	58 (48.3)	62 (51.7)		
Age, years				1.080	0.299
≤60	177	93 (52.5)	84 (47.5)		
≥60	191	90 (47.1)	101 (52.9)		
Ethnicity				2.532	0.282
Asian	158	79 (50.0)	79 (50.0)		
White	182	90 (49.5)	92 (50.5)		
Others	19	13 (68.4)	6 (31.6)		
BMI				0.019	0.890
≤24	160	77 (48.1)	83 (51.9)		
≥24	178	87 (48.9)	91 (51.1)		
Historical risk factors				0.324	0.850
Alcohol consumption	117	56 (47.9)	61 (52.1)		
Hepatitis virus	114	58 (40.3)	56 (59.7)		
Others	119	61 (51.3)	58 (48.7)		
Clinical stage				4.554	0.033
I, II	257	118 (45.9)	139 (54.1)		
III, IV	88	52 (59.1)	36 (40.9)		
T				3.983	0.046
T1, T2	275	130 (47.3)	145 (52.7)		
T3, T4	91	54 (59.3)	37 (40.7)		
N				-	0.622
N0	250	125 (50.0)	125 (50.0)		
N1	4	3 (75.0)	1 (25.0)		
M				0.970	0.622
M0	265	132 (49.8)	133 (50.2)		
M1	4	1 (25.0)	3 (75.0)		
Histologic grade				17.825	<0.01
G1, G2	232	96 (41.4)	136 (58.6)		
G3, G4	132	85 (64.4)	47 (35.6)		
AFP				24.348	<0.01
≤20	147	50 (34.0)[a]	97 (66.0)[a]		
≥20 and <400	66	36 (54.5)[b]	30 (45.5)[b]		
≥400	65	45 (69.2)[b]	20 (30.8)[b]		
Child pugh grade				1.499	0.221
A	217	89 (41.0)	128 (59.0)		
B, C	22	12 (54.5)	10 (45.5)		
Treatment type				0.610	0.435
Pharmaceutical therapy	184	88 (47.8)	96 (52.2)		
Radiation therapy	185	96 (51.9)	89 (48.1)		

BMI, body mass index; AFP, alpha-fetoprotein. Each superscript letter (a and b) denotes a subset of AFP categories whose RAB11B expression do not differ significantly from each other at the 0.05 significance level. No statistical differences exist between the same letter groups, but there are statistical differences between groups denoted by different letters.

dendritic cells (R=0.28, P=4.3x10^{-7}) (Fig. 5A). MK5 was also found to be positively associated with six types of cells of

Table III. Cox regression analysis of independent risk factors affecting the prognosis of patients with hepatocellular carcinoma.

A, The relationship between overall survival and clinicopathologic feature in patients with hepatocellular carcinoma using Univariate Cox regression.

Variable	Hazard ratio	95% confidence interval	P-value
Sex	1.303	0.849-1.997	0.225
Age	1.564	1.013-2.417	0.044
Body mass index	0.834	0.529-1.315	0.435
Race	2.317	1.358-3.954	0.002
Clinical stage	1.484	0.896-2.458	0.125
T	1.812	1.147-2.860	0.011
N	1.095	0.899-27.02	0.997
M	5.296	1.631-17.19	0.006
Histologic grade	1.269	0.817-1.973	0.288
AFP	2.063	1.194-3.564	0.009
Child pugh grade	1.577	0.711-3.499	0.262
Treatment type	1.289	0.843-1.970	0.241
Lnc-MAPKAPK5-AS1	1.039	1.002-1.078	0.039
MAPKAPK5	1.148	1.028-1.282	0.015

B, The relationship between overall survival and clinicopathologic feature in patients with hepatocellular carcinoma using Multivariate Cox regression.

Variable	Hazard ratio	95% confidence interval	P-value
Age	1.549	0.807-2.977	0.188
Race	1.613	0.744-3.499	0.255
T	1.122	0.386-2.058	0.787
M	4.184	2.297-4.515	0.002
AFP	1.577	0.758-3.280	0.222
lnc-MAPKAPK5-AS1	1.040	1.014-1.106	0.045
MAPKAPK5	1.219	1.031-1.495	0.029

AFP, alpha-fetoprotein.

the immune system (Fig. 5B). Furthermore, as suggested in Table V, MK5-AS1 expression is positively linked with multiple immune cell biomarkers in HCC. The aforementioned results demonstrated its effectiveness in regulating TME of HCC.

The immune cell infiltration ratio of TCGA-LIHC was evaluated based on CIBERSORT algorithm. Patients with HCC were divided according to the median of MK5-AS1 expression and the proportions of immune infiltrating cell subtypes in high and low expression groups were calculated (Fig. 5C). Using the R package 'GSVA', ssGSEA was used to calculate the abundance of immune cells based on the corresponding data set. For the majority of the 28 types of immune cells, including myeloid-derived suppressor cells, gamma delta T cells, effector memory $CD4^+$ T cells, mast cells, memory B cells and natural killer T cells were more significantly enriched in MK5-AS1 high expression group (Fig. 5D). The aforementioned findings indicated that MK5-AS1 may regulate the progression of HCC by affecting cellular infiltration of the immune system.

lnc-MAPKAPK5-AS1 expression is positively related to TMB and MSI in HCC. Inhibiting immune checkpoint signaling pathways are key strategies for the treatment of a range of cancers. The association of MK5-AS1 with ten common immune checkpoints in human cancers, including CD274, CTLA4, HAVCR2, LAG3, PDCD1, PDCD1LG2, TIGIT, SIGLEC15, ITPRIPL1 and IGSF8, was explored. The expression levels of six immune checkpoints were significantly increased in the MK5-AS1 high expression group (Fig. 6A).

As emerging markers of immunotherapy, the predictive value of TMB and MSI in certain cancers has been validated in clinical trials. The effects of TMB and MSI status on the expression level of MK5-AS1 were assessed using the Sangerbox database. Radar charts showed that the expression of MK5-AS1 was positively correlated with TMB and MSI in HCC (R=0.138, P=0.04; R=0.17, P=0.04, respectively) (Fig. 6B and C). The expression of MK5-AS1 revealed a significant effect on the TMB of patients with HCC in the analysis of data from TCGA (Fig. 6E). Collectively, these

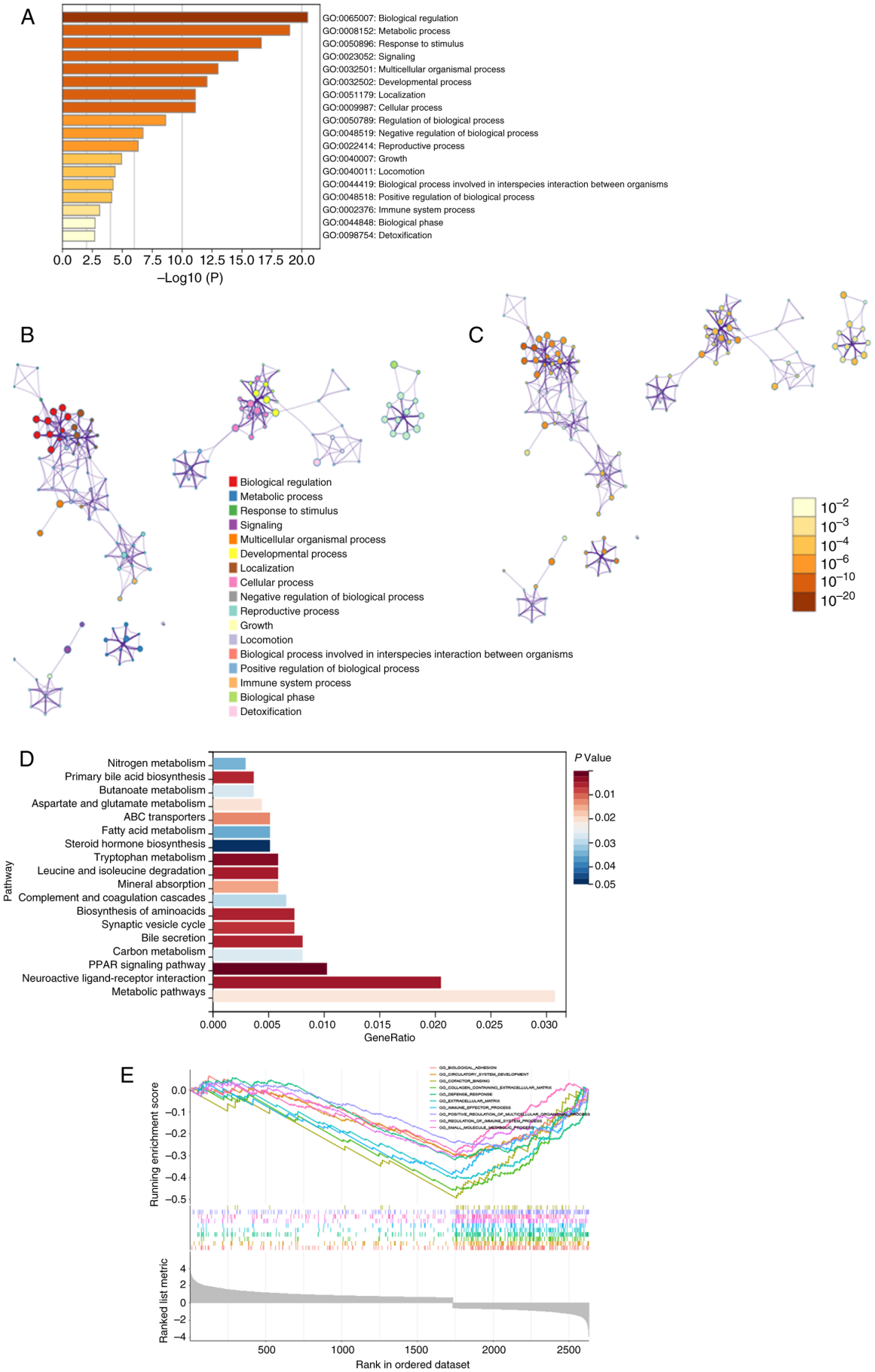

Figure 3. Signaling pathways enriched by GO, KEGG and GSEA. (A) GO analysis. (B) An interactive network of the enrichment terms colored by cluster. (C) An interactive network of the enrichment terms colored by P-value. (D) KEGG analysis. (E) The functional pathways enriched by GSEA analysis. GO, Gene Ontology; KEGG, Kyoto Encyclopedia of Genes and Genomes; GSEA, Gene Set Enrichment Analysis.

Table IV. Correlation analysis between MAPKAPK5 expression at protein level and clinicopathological feature in hepatocellular carcinoma.

Characteristics	n	Expression level of MAPKAPK5		χ^2	P-value
		High (n=24)	Low (n=66)		
Sex				0.256	1.000
Male	80	22 (27.5)	58 (72.5)		
Female	10	2 (20.0)	8 (80.0)		
Age, years				0.297	0.586
<60	71	18 (25.4)	53 (74.6)		
>60	19	6 (31.6)	13 (58.4)		
Pathology grade				5.415	0.074
I	4	0	4		
II	63	14 (22.2)	49 (77.8)		
III	23	10 (43.5)	13 (56.5)		
Tumor size(cm)				0.623	0.430
≤5	62	15 (24.2)	47 (75.8)		
>5	28	9 (32.1)	19 (67.9)		
Number of tumors				0.603	0.475
Single	79	20 (25.3)	59 (74.7)		
Multiple	11	4 (36.4)	7 (63.6)		
Liver cirrhosis nodules				1.553	0.224
≤1	9	4 (44.4)	5 (55.6)		
>1	86	20 (23.3)	66 (76.7)		
Tumor encapsulation				0.104	0.747
Complete	42	12 (28.6)	30 (71.4)		
Incomplete	47	12 (25.5)	35 (74.5)		
Clinical stage				7.701	0.017
I	85	20 (23.5)	65(76.5)		
II + III	5	4 (80.0)	1(20.0)		
T				0.173	0.677
T1	63	16 (25.4)	47 (74.6)		
T2 + T3	27	8 (29.6)	19 (70.4)		
Recurrence				0.001	0.974
Yes	49	13 (26.5)	36 (73.5)		
No	41	11 (26.8)	30 (73.2)		
HBsAg				1.904	0.274
Positive	70	17 (24.3)	53 (75.7)		
Negative	19	7 (36.8)	12 (63.2)		
HBcAb				0.043	1.000
Positive	80	20 (25.0)	60 (75.0)		
Negative	7	2 (28.6)	5 (71.4)		
Anti-Hepatitis C				0.342	0.558
Positive	1	0	1		
Negative	86	22 (25.6)	64 (74.4)		
T-Bil (μmol/l)				0.232	0.752
Medical reference value	76	21 (31.8)	55 (68.2)		
Abnormal value	14	3 (21.4)	11 (78.6)		
ALT (U/l)				5.011	0.025
Medical reference value	50	18 (36.0)	32 (64.0)		
Abnormal value	40	6 (15.0)	34 (85.0)		
AFP (μg/l)				0.691	0.406
≤20	36	8 (22.2)	28 (77.8)		
>20	53	16 (30.2)	37 (69.8)		

Table IV. Continued.

Characteristics	n	Expression level of MAPKAPK5		χ^2	P-value
		High (n=24)	Low (n=66)		
GGT (U/l)				0.135	0.701
≤40	31	9 (29.0)	22 (71.0)		
>40	59	15 (25.4)	44 (74.6)		
PD-L1 expression				7.003	0.008
Low	67	14 (20.9)	53 (79.1)		
High	17	9 (52.9)	8 (47.1)		
CTLA4 expression				0.174	0.677
Low	15	5 (33.3)	10 (66.7)		
High	68	19 (27.9)	49 (72.1)		

The medical reference value of T-Bil (μmol/l) and ALT (U/L) is 5.13-22.24, 7-40, respectively; Several variables have missing values in 90 specimens: 1 in tumor encapsulation and HBsAg, 3 in HBcAb, 3 in AntiHCV, 2 in T-Bil, 1 in ALT, 1 in AFP, 1 in GGT, 6 in PD-L1 and 7 in CTLA4. ALT, alanine aminotransferase; AFP, alpha-fetoprotein; GGT, gamma-glutamyl transpeptidase.

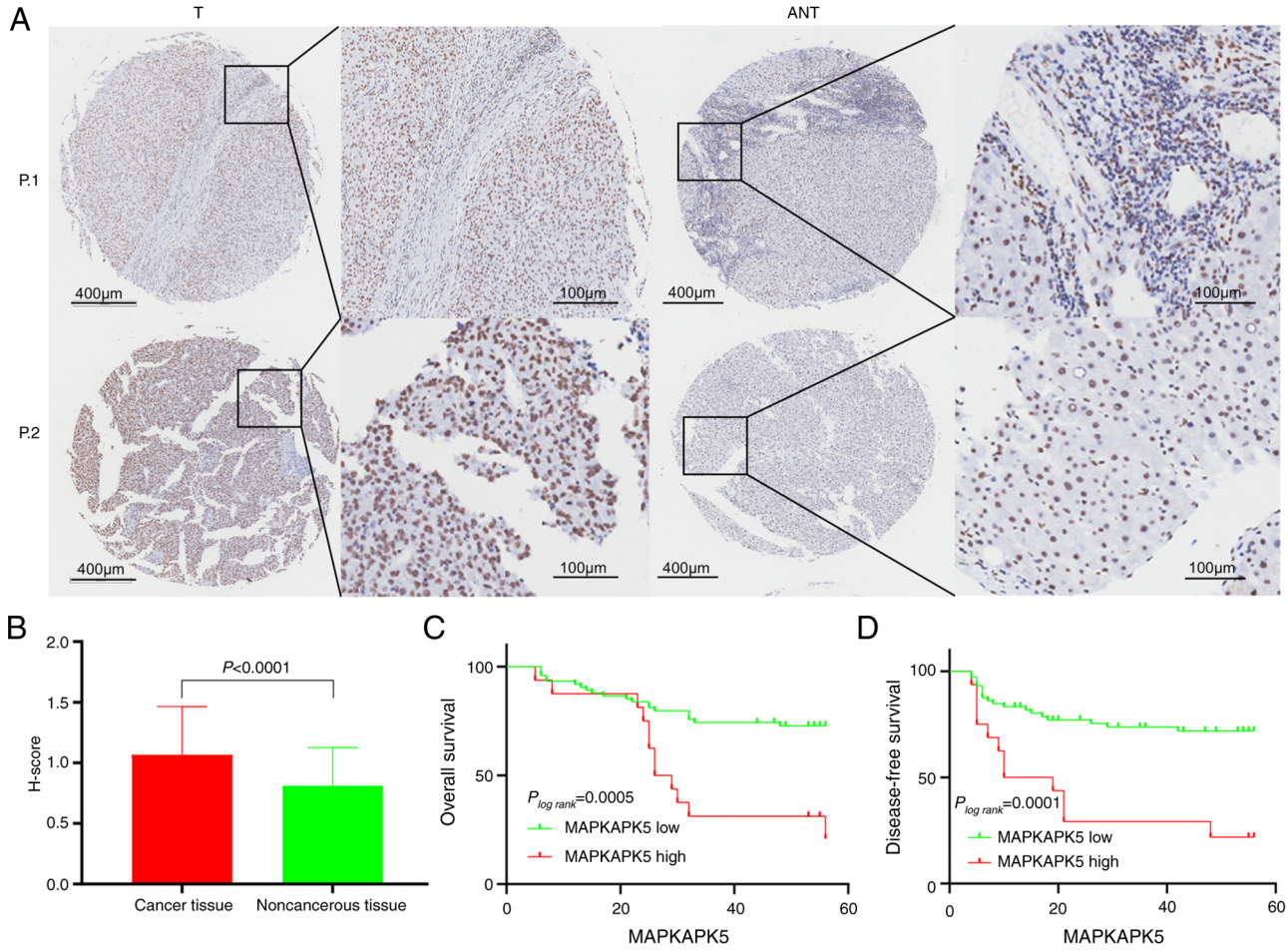

Figure 4. Immunohistochemical analysis of MAPKAPK5 protein in HCC. (A) Two pairs of representative immunohistochemical staining of MK5 in 90 cases of HCC, with magnification x100. (B) MK5 protein levels grouped by HCC and para-carcinoma tissues. (C and D) The relationship between MK5 expression and overall survival and disease-free survival in patients with HCC. HCC, hepatocellular carcinoma; T, tumor tissue; ANT, adjacent non-cancerous tissue.

findings suggested that the group with higher TMB may have a shorter survival time owing to the overexpression of MK5-AS1 in these patients with HCC.

Drug sensitivity analysis of lnc-MAPKAPK5-AS1. To further explore the clinical significance and drug sensitivity of MK5-AS1, based on 'pRRophetic' R package, the potential

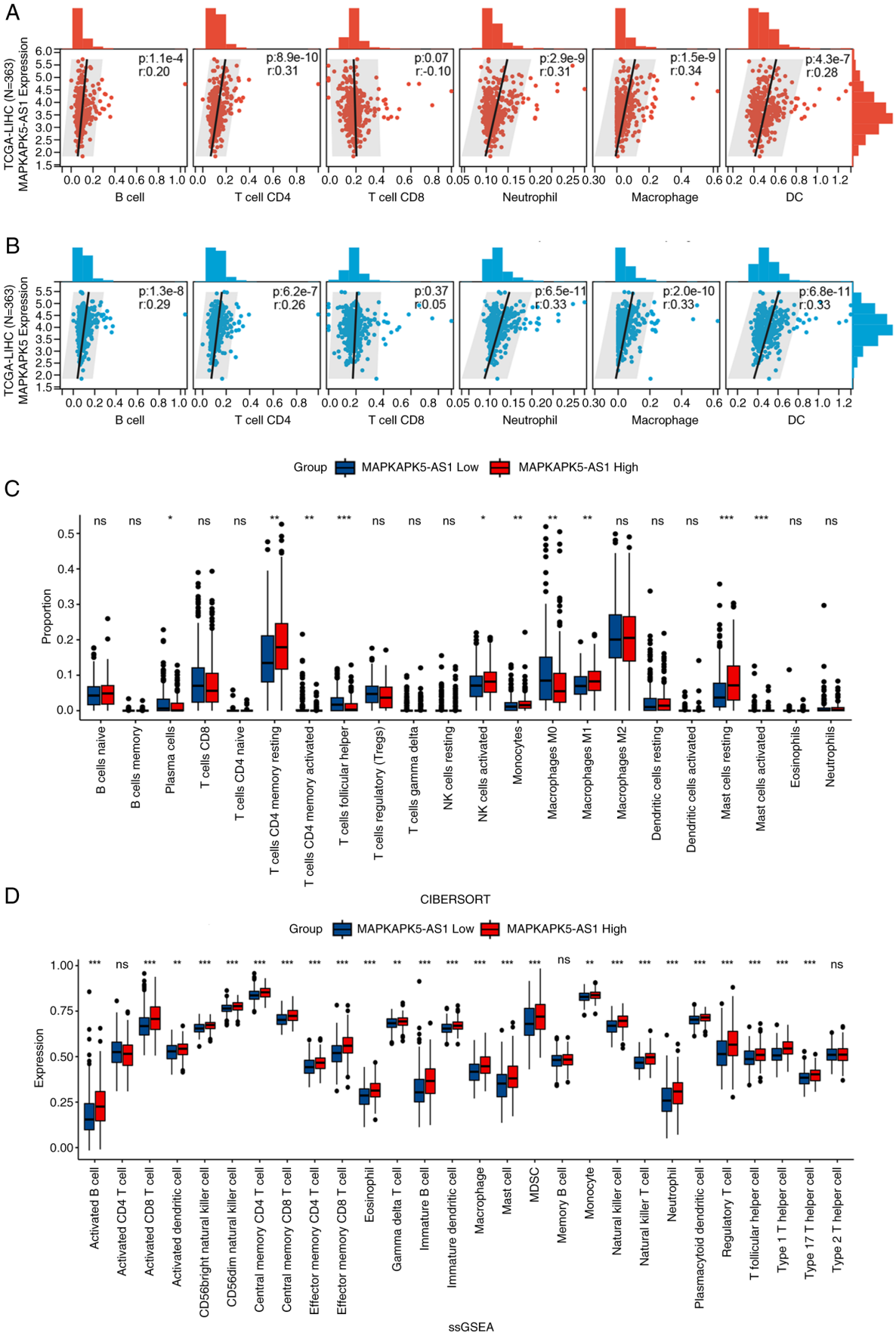

Figure 5. Correlation analysis of lnc-MAPKAPK5-AS1 expression and tumor microenvironment in HCC. (A) MK5-AS1 was positively linked with tumor immune cells infiltration levels of B cells, $CD8^+$ T cells, $CD4^+$ T cells, neutrophils and dendritic cells. (B) The relationships between MK5 and six types of cells of the immune system. (C) The box plot of 22 specific cells of the immune system exhibited by different groups by CIBERSORT. (D) Relationship between the expression of MK5-AS1 and 28 types of cells of the immune system in HCC by single sample Gene Set Enrichment Analysis. *P<0.05, **P<0.01 and ***P<0.001. HCC, hepatocellular carcinoma; TCGA-LIHC, The Cancer Genome Atlas Liver Hepatocellular Carcinoma; ns, not significant.

Table V. The relationship between lnc-MAPKAPK5-AS1 and biomarkers of immune system cells in hepatocellular carcinoma.

Immune cell	Biomarker	R-value	P-value
B cell	CD19	0.16	0.0022
	MS4A1	0.072	0.17
$CD4^+$ T cell	CD4	0.2	0.067
$CD8^+$ T cell	CD8A	0.11	0.013
	CD8B	0.12	0.02
Neutrophil	ITGAM	0.16	0.0016
	CD177	0.078	0.14
	CCR7	0.06	0.25
Dendritic cell	HLA-DRA	0.16	$6.6x10^{-4}$
	HLA-DRA1	0.16	0.054
	HLA-DPB1	0.077	0.14
	HLA-DQB1	0.13	0.015
	BDCA1	0.13	0.0049
	ITGAX	0.18	$6x10^{-4}$
	NRP1	0.17	0.0013
M1 macrophage	CD80	0.21	$4.7x10^{-6}$
	CD86	0.25	$3.4x10^{-8}$
	IL-1	0.091	0.047
M2 macrophage	CD163	0.097	0.034
	CD206	-0.092	0.044
	CD301	0.062	0.18

relationships between MK5-AS1 expression and drug sensitivity of targeted therapeutic drugs that commonly used in patients with HCC were further probed. Obviously, patients with low expression of MK5-AS1 were more sensitive to Axitinib, Bosutinib, Cyclopamine, dasatinib, Docetaxel, Embelin, Gefitinib, Lapatinib, Metformin, Methotrexate and Vorinostat. By contrast, the half-maximal inhibitory concentration (IC_{50}) calculated utilizing 'pRRophetic' R package of Bexarotene, Bleomycin, Cisplatin, Doxorubicin and Gemcitabine was lower in MK5-AS1 high expression group (Fig. 6D). These findings suggested that MK5-AS1 might act as an effective biomarker for the efficacy of targeted treatment of patients with HCC.

Mechanisms of lnc-MAPKAPK5-AS1 upregulation in HCC. To seek out the possible reasons for the upregulation of MK5-AS1 in HCC, the methylation level of promoter region near MK5-AS1 was analyzed based on sample type, clinical stage and histological grade and the mutation status of two genes in HCC was probed.

Firstly, the methylation data of the promoter region near MK5-AS1 was obtained using the Diseasemeth 2.0 database. The results revealed that methylation level in HCC tissues was significantly lower than that in normal tissues (Fig. 6F), and there were significant differences in the methylation expression level of MK5-AS1 in different clinical stages and histological grades of HCC (Fig. 6G and H), which provided evidence that the upregulation of MK5-AS1 in HCC might partly due to hypomethylation of its promoter. In addition, the overall result of the 'MAF' file was plotted and it was found that missense mutation accounted for the predominant part when the mutation types were classified according to different categories (Fig. 7A). Moreover, single nucleotide polymorphism appeared more frequently than insertions or deletions, with C>T being the most common mutation in single nucleotide variants. Then, the mutation status of MK5-AS1 and MK5 was explored using cBioPortal database, and the results showed that the incidence of MK5-AS1 mutation was 6% (21/360) in HCC, and only two of the 360 patients had missense mutation in MK5, demonstrating that this mutation is fairly unlikely to be the major reason of MK5-AS1 upregulation (Fig. S1A and B).

Prediction of miRNAs that probably interact with lnc-MAPKAPK5-AS1. Evidence suggests that lncRNAs in the cytoplasm can affect the stability and translation regulation of mRNA mainly through the ceRNA regulatory mechanism by adsorbing miRNAs. Using lncATLAS database, the expression pattern of MK5-AS1 in different cell lines was uncovered, while most of the data exhibited that MK5-AS1 is primarily located in the cytoplasm (Fig. 7B). Therefore, it was hypothesized that MK5-AS1 might promote the progression of HCC through the sponge adsorption of miRNAs. ENCORI database unveiled that four miRNAs (hsa-miR-452-5p, hsa-miR-556-3p, hsa-miR-4676-3p and hsa-miR-892c-3p) could directly bind to the gene body of MK5-AS1 and MK5. It has been already noted that hsa-miR-452-5p was overexpressed in HCC tissues compared with normal tissues, which lead to a poor prognosis of HCC through modulating the RNA levels of downstream target genes (35). Unfortunately, based on data from the LIRI-JP dataset of the ICGC database (https://dcc.icgc.org/, accessed on 10 January 2021) (36), there was no discernible variation in the expression pattern of these miRNAs between HCC tissues and normal tissues (Fig. S2A-D). Furthermore, there was no concomitant negative association between these miRNAs and the expression level of MK5-AS1 or MK5 owing to the limitation of sample size and data source (Fig. S2E-L); thus, further molecular experiments are required to confirm the specific mechanism.

Co-expression network construction and identification of immune-related key genes of HCC. A total of eight modules were generated in the hierarchical clustering tree (Fig. 7C). The correlations between all feature genes of these modules and CYT and IFNG6 scores reflecting immune activity are shown in Fig. 7D, in which the blue module showed the strongest association with the aforementioned two scores (R=0.75, P<0.001; R=0.61, P<0.001, Fig. 7F and G). Using MS>0.8 and GS>0.3, 15 genes (NCAPD2, TACC3, PRR11, TPX2, MFSD10, DBN1, ECT2, CENPF, NCAPH, CENPO, TICRR, CHEK1, SPINDOC, H2AX and TRIM59) were screened from the blue module as candidate hub genes. To further explore the biological function of these genes, a protein-protein interaction (PPI) network was constructed using the STRING database (Fig. 7E). Spearman's correlation analysis revealed strong correlation between genes and six types of cells of the immune system (Fig. 7H and I).

Discussion

Patients with HCC exhibited a poor survival and lack effective prognostic biomarkers over a long period of time. The

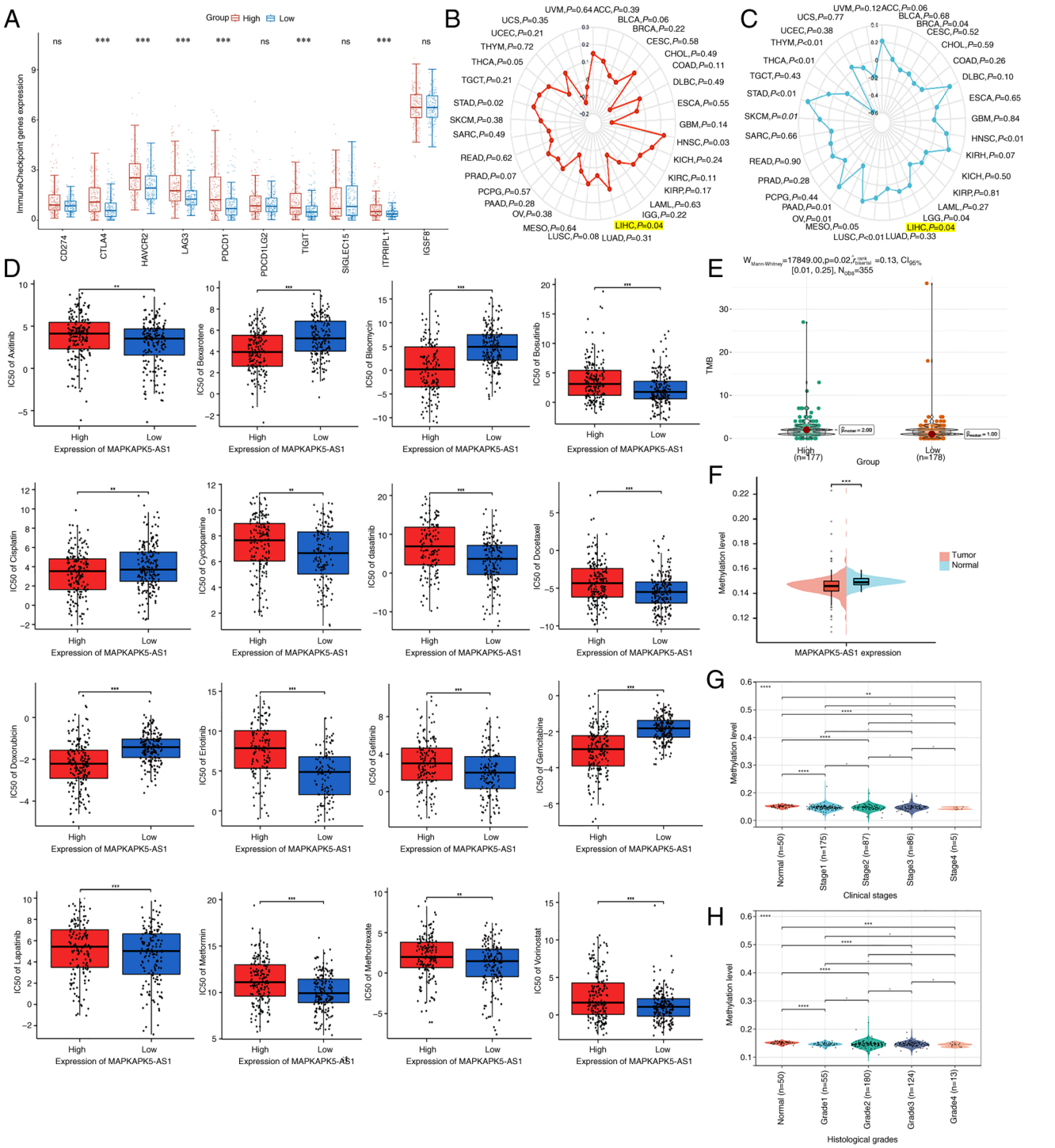

Figure 6. Visualization of ICIs, drug sensitivity and methylation status of lnc-MAPKAPK5-AS1 in HCC. (A) The expression distribution of ten immune-related genes in MK5-AS1 high and low groups. (B and C) Radar chart of the relationship between MK5-AS1 expression and microsatellite instability and ICIs. (D) Drug sensitivity analysis of MK5-AS1. (E) Comparison regarding the tumor mutational burden of MK5-AS1 high and low groups. (F) The methylation level of MK5-AS1 promoter between HCC tissues and normal tissues in The Cancer Genome Atlas. (G and H) The methylation level of MK5-AS1 promoter in different histologic grades and clinical stages. *P<0.05, **P<0.01, ***P<0.001 and ****P<0.0001. ICIs, immune checkpoint inhibitors; HCC, hepatocellular carcinoma.

identification of genes with potential value for the diagnosis and treatment of HCC will be critical to improving patient treatment. Studies have revealed that lncRNAs participate in gene regulation by acting as a miRNA sponge or RBP binding and play critical roles in tumor angiogenesis, invasion and metastasis (37-39). Antisense lncRNAs exhibit special structures and represent a class of lncRNAs that are complementary to other transcript sequences. lnc-MCM3AP-AS1 (40) and lnc-AFAP1-AS1 (41) may be novel molecular tumor markers. Previous research has demonstrated a role for MK5-AS1 in tumors. Cheng *et al* (42) demonstrated that MK5-AS1 may be a hypoxia-related lncRNA in HCC and involved in tumorigenesis and progression. Wang *et al* (43) constructed an immune-lncRNAs signature containing MK5-AS1

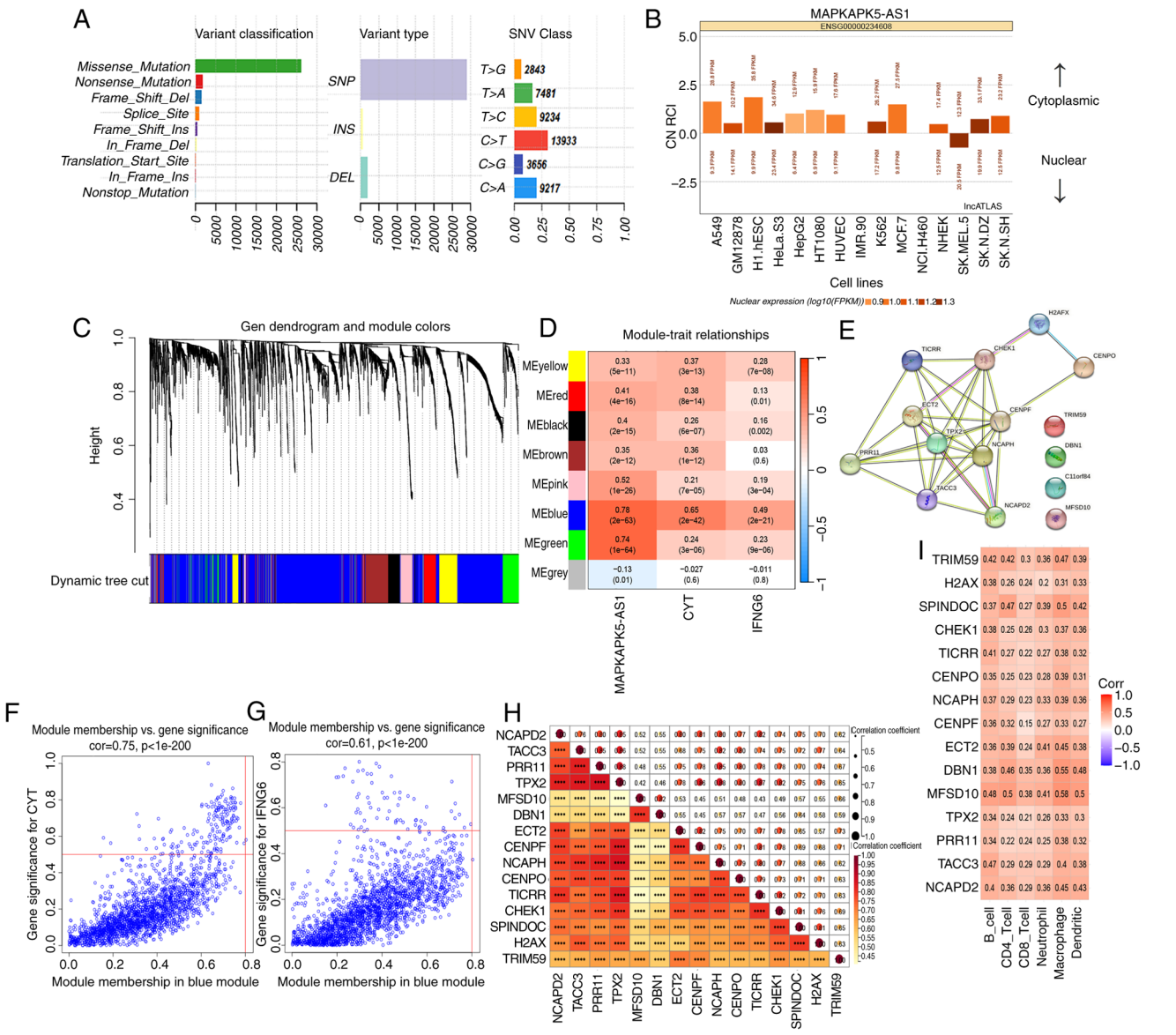

Figure 7. Identification of modules associated with immune activity through weighted correlation network analysis. (A) Types of mutations and single nucleotide variants classification in hepatocellular carcinoma. (B) MK5-AS1 is predicted to be mainly localized in the cytoplasm according to the analysis of lncATLAS database. (C) Gene dendrogram and module colors. (D) Heatmap of the relationship between module eigengenes and immunity. Each cell contained the correlation coefficient and P-value. (E) Protein-protein interaction network of hub genes. (F and G) Identification of modules related to clinical traits. (H) Correlation between 15 hub genes. (I) Correlation between hub genes and six types of cells of the immune system. ****P<0.0001.

in anaplastic gliomas. Several studies have revealed that MK5-AS1 may be acting as a ceRNA potential in various tumors (44-46).

Previous studies (7,8,46) on the role of MK5-AS1 in HCC were mostly focused on cell line experiments through reverse transcription-quantitative PCR and cell phenotype experiments and rarely integrated multiple large cancer databases such as TCGA, GEO and ICGC for overall analysis at the human tissue level. In the present study, a comprehensive bioinformatics analysis was performed using the aforementioned databases, including clinical correlation analysis, enrichment analysis, methylation analysis, immune infiltration analysis, association analysis with TMB and MSI, drug sensitivity analysis and gene mutation analysis. Core immune-related genes co-expressed with MK5-AS1 were screened by WGCNA analysis, and a PPI network was constructed to understand the reaction mechanism of gene expression regulation and biological signal transmission. Analysis of the external cohort of 90 patients with liver cancer verified that upregulated MK5-AS1 in liver cancer tissues was associated with poor prognosis of patients with HCC and revealed the potential positive regulatory relationship between MK5-AS1 and MK5. These findings provide substantial evidence of the functional role of MK5-AS1 in HCC.

Through data mining of TCGA and GEO, MK5-AS1 was found to be notably increased in HCC tissues and linked to poor outcome, suggesting that MK5-AS1 may be an independent prognostic factor in HCC. Unfavorable pathological grade, clinical stage, T stage and higher AFP was associated with the increased expression of MK5-AS1 and MK5 in HCC. A positive regulatory relationship between MK5-AS1 and its antisense transcript MK5 was also observed, which may

be involved in the progression of HCC; however, the specific mechanism remains to be elucidated. The protein expression of MK5 in HCC was significantly higher than that in adjacent non-cancerous tissues, which was in line with previous results. Correlation analysis revealed that advanced clinical stage, abnormal ALT value and upregulated PD-L1 expression was more frequent in the high MK5 group. ALT is a sensitive predictor of early hepatocyte injury and elevated ALT is associated with increased mortality of HCC (47). Patients in the TCGA and GSE144269 datasets were grouped by MK5-AS1 expression. DEG analysis and a Venn diagram were carried out to obtain intersection genes. In enrichment analysis, the FDR threshold of 0.25 is set based on a trade-off between statistics, the error rate of the actual study and the reliability of the results. This threshold not only guarantees a certain discovery rate, but also controls the error rate, which is a common balance point in genomics research. GO and KEGG analysis revealed that the DEGs may regulate the progression of HCC through pathways such as biological regulation, metabolic progress, response to stimulus, multicellular organismal process, immune system process, PRAK signaling pathway and cell adhesion molecules.

Cell adhesion molecules serve as the molecular foundation for a variety of critical physiological and pathological processes, including immunological response, inflammatory response, coagulation and tumor metastasis. ICAM-1/CD54 is expressed at low levels on resting vascular endothelial cells, increasing cell adhesion across HCC cells and endothelial cells by binding to particular receptors on their surface (48). Synaptic vesicles are involved in cellular component exchange, signal transduction and pathological progress, and some have even been linked to the TME (49). Fat is an important energy source and molecular signal. Dysmetabolism of fatty acids in the TME not only affects the susceptibility of patients with cancer to radiotherapy or chemotherapy, but also interferes with their immunotherapy by affecting the immune response of T cells (50). Regulation of immune system process, biological adhesion, collagen containing extracellular matrix, immune effector process and other pathways were enriched in GSEA analysis. These results suggest that MK5-AS1 is associated with multiple immune-related metabolic signal channels.

HCC is a tumor driven by chronic inflammation (51), and the immunosuppressive microenvironment of HCC is an important factor in disease progression. Current clinical studies have explored the complex interplay between NASH, HCC and the immune response, and numerous therapeutic approaches have focused on targeting immune cells. In particular, changes in B cells, T cells and dendritic cells in the adaptive immune system, impaired cytotoxicity of natural killer cells and the accumulation of neutrophils (52). To explore the specific mechanism of MK5-AS1 in immune regulation, immune infiltration data from TIMER was downloaded and it was found that MK5-AS1 was positively correlated with multiple types of immune system cells and corresponding biomarkers, suggesting that MK5-AS1 may negatively affect the prognosis of HCC owing to its regulatory role in the TME. The results of the present study indicated that MK5-AS1 was not directly involved in the functional regulation of $CD8^+$ T cells during certain stages or conditions of the immune response due to disparities in the specificity and regulatory mechanisms of gene expression. However, this does not mean that MK5-AS1 has no effect on $CD8^+$ T cells, because there may be indirect or conditional interactions; these possibilities should be further explored in future studies. Using the CIBERSORT and ssGSEA algorithm, plasma cells, T cells $CD4^+$ memory resting, macrophages M1 and several immune cells were found to be present at high levels in the MK5-AS1 high expression group. Previous research reported that patients with a higher proportion of plasma cells in HCC have a shorter survival time (53). Zong *et al* (54) demonstrated that M1 macrophages mediate inducible PD-L1 expression in HCC cells and perform a tumor-promoting role, which also lends credence to our conclusion.

As emerging biomarkers of cancer immunotherapy, TMB and MSI are closely related to clinical prognosis. TMB has been extensively utilized to forecast the effectiveness of immunotherapy in non-small cell lung cancer and melanoma, but few studies have focused on its role in HCC. In the present study, it was revealed that MK5-AS1 expression was positively related to TMB and MSI. Moreover, survival outcome was found in high TMB group verified by data in TCGA, which had higher expression of MK5-AS1. Immune checkpoints are pivotal effector molecules in the immune microenvironment. Currently, there are no well-established biomarkers for immunotherapy for tumors of the digestive system, especially for HCC. Under physiological conditions, PD-1 binds to PD-L1 to release inhibitory signals while CTLA-4 is present in regulatory T lymphocytes; they impede autoimmune responses and participate in the immune evasion process of HCC through various pathways (55,56). PD-L1 and TMB are not related in major tumor types such as HCC, head and neck squamous cell carcinoma, renal cell carcinoma and small cell lung cancer (57,58). Detection of both factors can provide guidance for the clinical treatment and application of ICIs (59). In non-small cell lung cancer, patients with both high PD-L1 expression and TMB exhibit the best curative effect from ICIs, with a clinical benefit rate of 50%, while patients with low PD-L1 expression and TMB have a clinical benefit rate of only 18.2% (60). In the present study, it was found that the PD-L1 and TMB levels of HCC in the high MK5-AS1 expression group were considerably increased compared with the low MK5-AS1 expression group, which is consistent with previous studies that revealed that HCC cases with a high TMB have a shorter OS (61,62). The infiltration of various types of immune system cells was also different between the two groups, indicating that TMB may also determine the efficacy of ICIs by affecting the TME of HCC. As a result, it would be a new challenge and strategy to screen the advantage groups or combination therapy for immunotherapy in the future.

To explore the mechanism of MK5-AS1 overexpression in HCC tissues, the mutation and methylation status of MK5-AS1 was examined. DNA methylation is an important form of epigenetic modification. Aberrant methylation affects the conformation of DNA, making it difficult for transcription factors to bind and inhibit gene transcription. Database prediction indicated that the methylation level of the MK5-AS1 promoter in HCC was lower than that in normal tissues and correlated with advanced clinical stage and histological grade, indicating that MK5-AS1 is upregulated in HCC tissues possibly from hypomethylation. Tao *et al* (63) previously confirmed

that MK5-AS1 expression in HBV-related HCC was elevated in M2 macrophages. As a result of N6-methyladenosine modification, the expression of MK5-AS1 in HCC cells was also increased after the transfer exosomes, which promotes cell proliferation.

WGCNA was applied to identify modules closely associated with immune scores in the MK5-AS1 high and low expression groups. Using MM and GS, 15 hub genes were screened out of the blue module, including TPX2, CENPO, CENPF and ECT2. Wang *et al* (64) demonstrated that TPX2 regulates CXCR5 through the NF-κB signaling pathway to improve the anti-tumor function of human $CD8^+$ T cells and has a synergistic effect with anti-PD-1 therapy. CENPO and CENPF are key genes related to antitumor immunity in HCC (65,66). Xu *et al* (67) reported that ECT2 promotes the polarization of M2 macrophages, which may be related to enhanced aerobic glycolysis.

In conclusion, the results of the present study revealed that the expression of MK5-AS1 was upregulated in HCC tissues and MK5-AS1 was co-expressed with its protein-coding gene MK5. Increased expression is linked to a poor prognosis as well as higher levels of immune infiltration and immune-related genes, indicating that MK5-AS1 may serve as a prognostic biomarker and therapeutic target for HCC.

Acknowledgements

Not applicable.

Funding

The present study was supported by the National Natural Science Foundation of China (grant no. 81803325), the Natural Science Foundation of Guangdong (grant nos. 2021A1515011175 and 2024A1515011646), the Guangzhou Science and Technology Project (grant no. 202102080126), the Key Project of Medicine Discipline of Guangzhou (grant no. 2025-2027-12), the Medical Science and Technology Foundation of Guangdong (grant no. A2024733) and the Basic Research Project of Key Laboratory of Guangzhou (grant no. 202102100001).

Availability of data and materials

The data generated in the present study may be requested from the corresponding author.

Authors' contributions

DWu and XH conceptualized the study, conducted investigation and wrote the original draft. Material preparation, data collection and analysis were performed by DWa, PQ, LZ, XH, BL and JC. DWu, DWa and PQ reviewed edited the manuscript. DWu and XH confirm the authenticity of all the raw data. All authors read and approved the final version of the manuscript.

Ethics approval and consent to participate

The present study was conducted in accordance with the Declaration of Helsinki, and was approved (approval no. SHYJS-CP-1901001 in 11th January 2019; and extended as approval no. SHYJS-BC-2310001 on 20th October, 2023) by the ethics committee of Shanghai Outdo Biotech Co., Ltd. (Shanghai, China).

Patient consent for publication

Not applicable.

Competing interests

The authors declare that they have no competing interests.

References

1. Xie DY, Ren ZG, Zhou J, Fan J and Gao Q: 2019 Chinese clinical guidelines for the management of hepatocellular carcinoma: Updates and insights. Hepatobiliary Surg Nutr 9: 452-463, 2020.
2. Xu XF, Xing H, Han J, Li ZL, Lau WY, Zhou YH, Gu WM, Wang H, Chen TH, Zeng YY, *et al*: Risk factors, patterns, and outcomes of late recurrence after liver resection for hepatocellular carcinoma: A multicenter study from China. JAMA Surg 154: 209-217, 2019.
3. Ahn JC, Lee YT, Agopian VG, Zhu Y, You S, Tseng HR and Yang JD: Hepatocellular carcinoma surveillance: Current practice and future directions. Hepatoma Res 8: 10, 2022.
4. Mercer TR, Dinger ME and Mattick JS: Long non-coding RNAs: Insights into functions. Nat Rev Genet 10: 155-159, 2009.
5. Luo S, Lu JY, Liu L, Yin Y, Chen C, Han X, Wu B, Xu R, Liu W, Yan P, *et al*: Divergent lncRNAs regulate gene expression and lineage differentiation in pluripotent cells. Cell Stem Cell 18: 637-652, 2016.
6. Wang H, Shi Y, Chen CH, Wen Y, Zhou Z, Yang C, Sun J, Du G, Wu J, Mao X, *et al*: KLF5-induced lncRNA IGFL2-AS1 promotes basal-like breast cancer cell growth and survival by upregulating the expression of IGFL1. Cancer Lett 515: 49-62, 2021.
7. Ji H, Hui B, Wang J, Zhu Y, Tang L, Peng P, Wang T, Wang L, Xu S, Li J and Wang K: Long noncoding RNA MAPKAPK5-AS1s promotes colorectal cancer proliferation by partly silencing p21 expression. Cancer Sci 110: 72-85, 2019.
8. Yang T, Chen WC, Shi PC, Liu MR, Jiang T, Song H, Wang JQ, Fan RZ, Pei DS and Song J: Long noncoding RNA MAPKAPK5-AS1 promotes colorectal cancer progression by cis-regulating the nearby gene MK5 and acting as a let-7f-1-3p sponge. J Exp Clin Cancer Res 39: 139, 2020.
9. Zhang H, Wang Y and Lu J: Identification of lung-adenocarcinoma-related long non-coding RNAs by random walking on a competing endogenous RNA network. Ann Transl Med 7: 339, 2019.
10. Gao GF, Parker JS, Reynolds SM, Silva TC, Wang LB, Zhou W, Akbani R, Bailey M, Balu S, Berman BP, *et al*: Before and after: Comparison of legacy and harmonized TCGA genomic data commons' data. Cell Syst 9: 24-34.e10, 2019.
11. Barrett T, Wilhite SE, Ledoux P, Evangelista C, Kim IF, Tomashevsky M, Marshall KA, Phillippy KH, Sherman PM, Holko M, *et al*: NCBI GEO: Archive for functional genomics data sets-update. Nucleic Acids Res 41(Database issue): D991-D995, 2013.
12. Zhou Y, Zhou B, Pache L, Chang M, Khodabakhshi AH, Tanaseichuk O, Benner C and Chanda SK: Metascape provides a biologist-oriented resource for the analysis of systems-level datasets. Nat Commun 10: 1523, 2019.
13. Newman AM, Liu CL, Green MR, Gentles AJ, Feng W, Xu Y, Hoang CD, Diehn M and Alizadeh AA: Robust enumeration of cell subsets from tissue expression profiles. Nat Methods 12: 453-457, 2015.
14. Subramanian A, Tamayo P, Mootha VK, Mukherjee S, Ebert BL, Gillette MA, Paulovich A, Pomeroy SL, Golub TR, Lander ES and Mesirov JP: Gene set enrichment analysis: A knowledge-based approach for interpreting genome-wide expression profiles. Proc Natl Acad Sci USA 102: 15545-15550, 2005.
15. Li H, Liu C, Huang S, Wang X, Cao M, Gu T, Ou X, Pan S, Lin Z, Wang X, *et al*: Multi-omics analyses demonstrate the modulating role of gut microbiota on the associations of unbalanced dietary intake with gastrointestinal symptoms in children with autism spectrum disorder. Gut Microbes 15: 2281350, 2023.

16. Song J, Ren K, Zhang D, Lv X, Sun L, Deng Y and Zhu H: A novel signature combing cuproptosis- and ferroptosis-related genes in sepsis-induced cardiomyopathy. Front Genet 14: 1170737, 2023.
17. Rukhsana, Supty AT, Hussain M and Lee Y: STK3 higher expression association with clinical characteristics in intrinsic subtypes of breast cancer invasive ductal carcinoma patients. Breast Cancer Res Treat 206: 119-129, 2024.
18. Reimand J, Isserlin R, Voisin V, Kucera M, Tannus-Lopes C, Rostamianfar A, Wadi L, Meyer M, Wong J, Xu C, *et al*: Pathway enrichment analysis and visualization of omics data using g:Profiler, GSEA, cytoscape and EnrichmentMap. Nat Protoc 14: 482-517, 2019.
19. Li T, Fan J, Wang B, Traugh N, Chen Q, Liu JS, Li B and Liu XS: TIMER: A web server for comprehensive analysis of tumor-infiltrating immune cells. Cancer Res 77: e108-e110, 2017.
20. Samstein RM, Lee CH, Shoushtari AN, Hellmann MD, Shen R, Janjigian YY, Barron DA, Zehir A, Jordan EJ, Omuro A, *et al*: Tumor mutational load predicts survival after immunotherapy across multiple cancer types. Nat Genet 51: 202-206, 2019.
21. Klein O, Kee D, Markman B, Carlino MS, Underhill C, Palmer J, Power D, Cebon J and Behren A: Evaluation of TMB as a predictive biomarker in patients with solid cancers treated with anti-PD-1/CTLA-4 combination immunotherapy. Cancer Cell 39: 592-593, 2021.
22. Goodman AM, Kato S, Bazhenova L, Patel SP, Frampton GM, Miller V, Stephens PJ, Daniels GA and Kurzrock R: Tumor mutational burden as an independent predictor of response to immunotherapy in diverse cancers. Mol Cancer Ther 16: 2598-2608, 2017.
23. Feng D, Hui X, Shi-Chun L, Yan-Hua B, Li C, Xiao-Hui L and Jie-Yu Y: Initial experience of anti-PD1 therapy with nivolumab in advanced hepatocellular carcinoma. Oncotarget 8: 96649-96655, 2017.
24. Geeleher P, Cox NJ and Huang RS: Clinical drug response can be predicted using baseline gene expression levels and in vitro drug sensitivity in cell lines. Genome Biol 15: R47, 2014.
25. Maeser D, Gruener RF and Huang RS: oncoPredict: An R package for predicting in vivo or cancer patient drug response and biomarkers from cell line screening data. Brief Bioinform 22: bbab260, 2021.
26. Xiong Y, Wei Y, Gu Y, Zhang S, Lyu J, Zhang B, Chen C, Zhu J, Wang Y, Liu H and Zhang Y: DiseaseMeth version 2.0: A major expansion and update of the human disease methylation database. Nucleic Acids Res 45(D1): D888-D895, 2017.
27. Gao J, Aksoy BA, Dogrusoz U, Dresdner G, Gross B, Sumer SO, Sun Y, Jacobsen A, Sinha R, Larsson E, *et al*: Integrative analysis of complex cancer genomics and clinical profiles using the cBioPortal. Sci Signal 6: pl1, 2013.
28. Mas-Ponte D, Carlevaro-Fita J, Palumbo E, Hermoso Pulido T, Guigo R and Johnson R: LncATLAS database for subcellular localization of long noncoding RNAs. RNA 23: 1080-1087, 2017.
29. Li JH, Liu S, Zhou H, Qu LH and Yang JH: starBase v2.0: Decoding miRNA-ceRNA, miRNA-ncRNA and protein-RNA interaction networks from large-scale CLIP-Seq data. Nucleic Acids Res 42(Database issue): D92-D97, 2014.
30. Langfelder P and Horvath S: WGCNA: An R package for weighted correlation network analysis. BMC Bioinformatics 9: 559, 2008.
31. Szklarczyk D, Morris JH, Cook H, Kuhn M, Wyder S, Simonovic M, Santos A, Doncheva NT, Roth A, Bork P, *et al*: The STRING database in 2017: Quality-controlled protein-protein association networks, made broadly accessible. Nucleic Acids Res 45: D362-D368, 2017.
32. Wakiyama H, Masuda T, Motomura Y, Hu Q, Tobo T, Eguchi H, Sakamoto K, Hirakawa M, Honda H and Mimori K: Cytolytic activity (CYT) score is a prognostic biomarker reflecting host immune status in hepatocellular Carcinoma (HCC). Anticancer Res 38: 6631-6638, 2018.
33. Seiwert TY, Burtness B, Mehra R, Weiss J, Berger R, Eder JP, Heath K, McClanahan T, Lunceford J, Gause C, *et al*: Safety and clinical activity of pembrolizumab for treatment of recurrent or metastatic squamous cell carcinoma of the head and neck (KEYNOTE-012): An open-label, multicentre, phase 1b trial. Lancet Oncol 17: 956-965, 2016.
34. Chandrashekar DS, Karthikeyan SK, Korla PK, Patel H, Shovon AR, Athar M, Netto GJ, Qin ZS, Kumar S, Manne U, *et al*: UALCAN: An update to the integrated cancer data analysis platform. Neoplasia 25: 18-27, 2022.
35. Zheng Z, Liu J, Yang Z, Wu L, Xie H, Jiang C, Lin B, Chen T, Xing C, Liu Z, *et al*: MicroRNA-452 promotes stem-like cells of hepatocellular carcinoma by inhibiting Sox7 involving Wnt/β-catenin signaling pathway. Oncotarget 7: 28000-28012, 2016.
36. Bertucci F, Chaffanet M and Birnbaum D: An ICGC major achievement in breast cancer: A comprehensive catalog of mutations and mutational signatures. Chin Clin Oncol 6: 4, 2017.
37. Li Z, Lin Y, Cheng B, Zhang Q and Cai Y: Identification and analysis of potential key genes associated with hepatocellular carcinoma based on integrated bioinformatics methods. Front Genet 12: 571231, 2021.
38. Cui XY, Zhan JK and Liu YS: Roles and functions of antisense lncRNA in vascular aging. Ageing Res Rev 72: 101480, 2021.
39. Wang J, Su Z, Lu S, Fu W, Liu Z, Jiang X and Tai S: LncRNA HOXA-AS2 and its molecular mechanisms in human cancer. Clin Chim Acta 485: 229-233, 2018.
40. Wang Y, Yang L, Chen T, Liu X, Guo Y, Zhu Q, Tong X, Yang W, Xu Q, Huang D and Tu K: A novel lncRNA MCM3AP-AS1 promotes the growth of hepatocellular carcinoma by targeting miR-194-5p/FOXA1 axis. Mol Cancer 18: 28, 2019.
41. Zhang JY, Weng MZ, Song FB, Xu YG, Liu Q, Wu JY, Qin J, Jin T and Xu JM: Long noncoding RNA AFAP1-AS1 indicates a poor prognosis of hepatocellular carcinoma and promotes cell proliferation and invasion via upregulation of the RhoA/Rac2 signaling. Int J Oncol 48: 1590-1598, 2016.
42. Cheng M, Zhang J, Cao PB and Zhou GQ: Prognostic and predictive value of the hypoxia-associated long non-coding RNA signature in hepatocellular carcinoma. Yi Chuan 44: 153-167, 2022.
43. Wang W, Zhao Z, Yang F, Wang H, Wu F, Liang T, Yan X, Li J, Lan Q, Wang J and Zhao J: An immune-related lncRNA signature for patients with anaplastic gliomas. J Neurooncol 136: 263-271, 2018.
44. Zhang J, Fan D, Jian Z, Chen GG and Lai PB: Cancer specific long noncoding RNAs show differential expression patterns and competing endogenous RNA potential in hepatocellular carcinoma. PLoS One 10: e0141042, 2015.
45. Yang J, Xu QC, Wang ZY, Lu X, Pan LK, Wu J and Wang C: Integrated analysis of an lncRNA-associated ceRNA network reveals potential biomarkers for hepatocellular carcinoma. J Computat Biol 28: 330-344, 2021.
46. Peng Z, Ouyang X, Wang Y and Fan Q: MAPKAPK5-AS1 drives the progression of hepatocellular carcinoma via regulating miR-429/ZEB1 axis. BMC Mol Cell Biol 23: 21, 2022.
47. Wedemeyer H, Hofmann WP, Lueth S, Malinski P, Thimme R, Tacke F and Wiegand J: (ALT screening for chronic liver diseases: Scrutinizing the evidence). Z Gastroenterol 48: 46-55, 2010 (In German).
48. Han P, Lei Y, Liu J, Liu J, Huang H, Tian D and Yan W: Cell adhesion molecule BVES functions as a suppressor of tumor cells extrusion in hepatocellular carcinoma metastasis. Cell Commun Signal 20: 149, 2022.
49. Xu Y, Feng K, Zhao H, Di L, Wang L and Wang R: Tumor-derived extracellular vesicles as messengers of natural products in cancer treatment. Theranostics 12: 1683-1714, 2022.
50. Luu M, Riester Z, Baldrich A, Reichardt N, Yuille S, Busetti A, Klein M, Wempe A, Leister H, Raifer H, *et al*: Microbial short-chain fatty acids modulate CD8(+) T cell responses and improve adoptive immunotherapy for cancer. Nat Commun 12: 4077, 2021.
51. Ringelhan M, Pfister D, O'Connor T, Pikarsky E and Heikenwalder M: The immunology of hepatocellular carcinoma. Nat Immunol 19: 222-232, 2018.
52. Gregory SN, Perati SR and Brown ZJ: Alteration in immune function in patients with fatty liver disease. Hepatoma Res 8: 31, 2022.
53. Zhang S, Liu Z, Wu D, Chen L and Xie L: Single-Cell RNA-Seq analysis reveals microenvironmental infiltration of plasma cells and hepatocytic prognostic markers in HCC with Cirrhosis. Front Oncol 10: 596318, 2020.
54. Zong Z, Zou J, Mao R, Ma C, Li N, Wang J, Wang X, Zhou H, Zhang L and Shi Y: M1 macrophages induce PD-L1 expression in hepatocellular carcinoma cells through IL-1β signaling. Front Immunol 10: 1643, 2019.
55. Yao S and Chen L: PD-1 as an immune modulatory receptor. Cancer J 20: 262-264, 2014.
56. Chen X, Du Y, Hu Q and Huang Z: Tumor-derived CD4+CD25+regulatory T cells inhibit dendritic cells function by CTLA-4. Pathol Res Pract 213: 245-249, 2017.
57. Rizvi H, Sanchez-Vega F, La K, Chatila W, Jonsson P, Halpenny D, Plodkowski A, Long N, Sauter JL, Rekhtman N, *et al*: Molecular determinants of response to anti-programmed cell death (PD)-1 and anti-programmed death-ligand 1 (PD-L1) blockade in patients with non-small-cell lung cancer profiled with targeted next-generation sequencing. J Clin Oncol 36: 633-641, 2018.

58. Yarchoan M, Albacker LA, Hopkins AC, Montesion M, Murugesan K, Vithayathil TT, Zaidi N, Azad NS, Laheru DA, Frampton GM and Jaffee EM: PD-L1 expression and tumor mutational burden are independent biomarkers in most cancers. JCI Insight 4: e126908, 2019.
59. Yarchoan M, Hopkins A and Jaffee EM: Tumor mutational burden and response rate to PD-1 inhibition. N Engl J Med 377: 2500-2501, 2017.
60. Jiang J, Jin Z, Zhang Y, Peng L, Zhang Y, Zhu Z, Wang Y, Tong D, Yang Y, Wang J, *et al*: Robust prediction of immune checkpoint inhibition therapy for non-small cell lung cancer. Front Immunol 12: 646874, 2021.
61. Cai H, Zhang Y, Zhang H, Cui C, Li C and Lu S: Prognostic role of tumor mutation burden in hepatocellular carcinoma after radical hepatectomy. J Surg Oncol 121: 1007-1014, 2020.
62. Huo J, Wu L and Zang Y: A prognostic model of 15 immune-related gene pairs associated with tumor mutation burden for hepatocellular carcinoma. Front Mol Biosci 7: 581354, 2020.
63. Tao L, Li D, Mu S, Tian G and Yan G: LncRNA MAPKAPK5_AS1 facilitates cell proliferation in hepatitis B virus -related hepatocellular carcinoma. Lab Invest 102: 494-504, 2022.
64. Wang X, Wang J, Shen H, Luo Z and Lu X: Downregulation of TPX2 impairs the antitumor activity of CD8+ T cells in hepatocellular carcinoma. Cell Death Dis 13: 223, 2022.
65. He K, Xie M, Li J, He Y and Yin Y: CENPO is associated with immune cell infiltration and is a potential diagnostic and prognostic marker for hepatocellular carcinoma. Int J Gen Med 15: 7493-7510, 2022.
66. Si T, Huang Z, Jiang Y, Walker-Jacobs A, Gill S, Hegarty R, Hamza M, Khorsandi SE, Jassem W, Heaton N and Ma Y: Expression levels of three key genes CCNB1, CDX20, and CENPF in HCC are associated with antitumor Immunity. Front Oncol 11: 738841, 2021.
67. Xu D, Wang Y, Wu J, Zhang Z, Chen J, Xie M, Tang R, Chen C, Chen L, Lin S, *et al*: ECT2 overexpression promotes the polarization of tumor-associated macrophages in hepatocellular carcinoma via the ECT2/PLK1/PTEN pathway. Cell Death Dis 12: 162, 2021.